

Article - Human and Animal Health

Bixinoids Derived from *Bixa orellana* as a Potential Zika Virus Inhibitor Using Molecular Simulations. Antiviral Effect on the Zika Virus of Bixinoids

Antonio Carlos Nogueira Sobrinho^{1,2*}
<http://orcid.org/0000-0002-9921-3350>

Caio Henrique Alexandre Roberto³
<https://orcid.org/0000-0001-7590-5830>

Danielle Malta Lima¹
<https://orcid.org/0000-0002-1899-7238>

Aluisio Marques da Fonseca⁴
<https://orcid.org/0000-0002-8112-9513>

Emmanuel Silva Marinho³
<https://orcid.org/0000-0002-4774-8775>

¹University of Fortaleza, Graduate Program in Medical Sciences, Fortaleza, Ceará, Brazil; ²State University of Ceará, Faculty of Education, Science and Letters of Iguatu, Iguatu, Ceará, Brazil; ³State University of Ceará, Faculty of Philosophy Dom Aureliano Matos, Limoeiro do Norte, Ceará, Brazil; ⁴University of International Integration of Afro-Brazilian Lusophony, Department of Clinical and Toxicological Analysis, Redenção, Ceará, Brazil.

Editor-in-Chief: Alexandre Rasi Aoki

Associate Editor: Daniel Fernandes

Received: 20-Jan-2021; Accepted: 08-Oct-2021.

*Correspondence: caiosobrinho@yahoo.com.br (A.C.N.S.).

HIGHLIGHTS

- Zika virus non-structural proteins are important pharmacological targets.
- Bixin and derived molecules interact with non-structural proteins.
- Bixin and ethyl bixin has the potential to interfere with the viral replication mechanism.
- Bixin and ethyl bixin an indicative of being a promising anti-Zika agent.

Abstract: Zika fever is a viral infection of great relevance in public health, especially in tropic regions, in which there is a predominance of mosquitoes of the genus *Aedes*, vectors of the disease. Microcephaly in neonatal children and Guillain-Barré syndrome in adults can be caused by the action of the Zika virus (ZIKV). Non-structural proteins, such as NS2B, NS3 and NS5, are important pharmacological targets, due to their action in the life cycle. The absence of anti-Zika drugs raises new research, including prospecting for natural products. This work investigated the *in silico* antiviral activity of bixin and six other derived molecules against the Zika viral proteins NS2B-NS3 and NS5. The optimized structure was subjected to molecular docking to

characterize the interaction between bixinoids and ZIKV non-structural proteins, where significant interactions were observed with amino acid residues in the catalytic site in each enzyme. These results suggest that bixin and ethyl bixin has the potential to interfere with the enzymatic activity of NS2B, NS3 and NS5, thus being an indication of being a promising anti-Zika agent.

Keywords: *Bixa orellana*; Flavivirus; Docking Molecular; NS2B-NS3; NS5.

INTRODUCTION

Zika fever is a viral infection caused by the Zika virus (ZIKV), belonging to the family *Flaviviridae*, genus *Flavivirus*, transmitted by the bite of female mosquitoes of the genus *Aedes* [1]. Considered a pathogen of importance in public health, ZIKV has been responsible in recent years for neurological disorders in a considerable percentage of patients, in addition can trigger Guillain-Barré syndrome [2] and cases of microcephaly in fetuses and newborn children [3].

The first report of infection occurred in 1947 in the Zika Forest in Uganda, Africa from rhesus monkeys. In 2007 an epidemic was reported in the Micronesia region on the island Yap [4], followed by another epidemic between the years 2013-2014 in French Polynesia, also in Oceania [5]. On the American continent, there was the first record on Easter Island, 3700 km from the west coast of Chile, with indigenous transmission [6]. In Brazil, the first autochthonous cases were reported and subsequently identified since late 2014 and early 2015 [7, 8].

ZIKV has an RNA genome, single-stranded, positive-sense, encoding a single polyprotein, later cleaved by host cell proteases and by the NS2B and NS3 viral proteases themselves. The cleavage products generate the three structural proteins (C, prM / M, and E) and the seven non-structural proteins (NS1, NS2A, NS2B, NS3, NS4A, NS4B, and NS5), important in the processes of infection, maturation, and replication [9, 10]. The NS2B-NS3 and NS5 proteases are an important pharmacological target due to its key role in the ZIKV life cycle.

Bixa orellana L. is a plant native to tropical America, whose seeds (annatto) have been used since the pre-colonial period by the indigenous peoples, for the extraction of pigments used in religious and cultural rituals, as a repellent and to treat diseases [11]. Bixinoids were a chemical group of apocarotenoid-type pigments, widely used in the cosmetics and food industry [12].

Bixin is a dicarboxylic monomethyl ester apocarotenoid, with molecular formula $C_{25}H_{30}O_4$, mass of 394.503 Da and mass of the monoisotopic of 394.214417 Da, extracted from the seeds of the native Brazilian plant species *Bixa orellana* L., whose pigment provides a range of colors composed of red, orange, and yellow tones. This group of carotenoid pigments has ethnomedicinal use among traditional Latin American peoples [13]. Bixinoids are bioactive compounds indicative of medicinal action, including antiviral effect [14, 15]. Reports of the use of medicinal plants by traditional communities are strong indications of biological action and the presence of bioactive molecules. The ethnomedicinal use of annatto seeds, associated with reports in the literature of antiviral action, prompted this study of *in silico* activity.

There is no specific approved treatment for ZIKV infection, only guidelines from the Centers for Disease Control and Prevention (CDC) for the treatment of symptoms, hydration, rest, and use of paracetamol for fever and pain. As for preventive measures by immunizing the population, the vaccines under development are still in clinical phase I and II studies [16].

The absence of drugs and effective immunobiologicals in the management of ZIKV infection raises new studies of molecular prospecting of substances with bioactivity against pharmacological targets of ZIKV, such as NS2B-NS3 and NS5 proteins. Thus, this study aims to investigate the antiviral potential of bixinoids through molecular docking with non-structural proteins of the ZIKV.

MATERIALS AND METHOD

Computational details

The molecular docking simulations were performed on the Windows 10 64-bit software operating system. The software used, UCSF Chimera™ [17], Autodocktools™ [18], AutoDockVina™ [19], Avogadro™ (<http://avogadro.cc/>), Discovery studio visualizer™ viewer [20] and Marvin™ 19.8, 2020, (<http://www.chemaxon.com>), Ligplot™ [21]. They are all free of charge for academic use.

Obtaining structures and optimization

The two-dimensional structures of the annatto bixinoids (ID5020631), bixin (ID4444638), crocetin dimethyl ester (4475264), ethyl bixin (4940995), mycorradicin (4948234), norbixin (4444661) and transcrocetin (4444644), were found in the repository of the structures in the repository chemspider (<http://www.chemspider.com/>) and drawn in the MarvinSketch™ software. The structural coordinates obtained from the repository were optimized geometrically (lowest energy state) using the classic MMFF94 force field formalism (Merck Molecular Force Field 94) [22] with descending steepest algorithm [23] with cycles of 50 interactions. All optimization calculations were performed on the Avogadro code [24].

Protein Preparation

To obtain the protein structure of the NS2B-NS3 (5lc0) and NS5 (5m5b) of the zika virus, the virtual protein data bank (PDB) repository (<https://www.rcsb.org/>) was used. Then, using the UCSF Chimera™ software [17], polar hydrogens were added, the protein structure was visualized, and the residues cleaned, so that there was no interference between interactions. Finally, the target proteins were in PDBQT.

Docking analysis

The interactions of molecular docking of bixinoids with the NS2B-NS3 protein using the resources available in Autodock vina, using a Lamarckian genetic algorithm, it is possible to define the grid box parameters, configured: *Center_x* = 78.317, *center_y* = 53.991, *center_z* = 152.138, *size_x* = 94, *size_y* = 76, *size_z* = 72, *spacing* = 0.589 e *exhaustiveness* = 8.

The grid box parameters used for the NS5 protein follow: *Center_x* = 0.725, *center_y* = 21.120, *center_z* = 72.094, *size_x* = 126, *size_y* = 126, *size_z* = 126, *spacing* = 0.624 e *exhaustiveness* = 8.

The docking results were clustered into groups with RMSD (Root-mean-square deviation) lower than 2.0 Å [25]. To guarantee the docking validity, a redocking procedure was carried out in the same Auto Dock Vina™ software [26] under the same conditions shown above, using the native ligands of the PDB structure [27] and the types of chemical interactions L-R's were analysed and the maps were generated using the Discovery Studio™ software.

In silico test of ADME properties

To conduct the drugability profile of bixinoids, the molecules were subjected to drug-likeness screening on the SwissADME (<http://www.swissadme.ch/>) [28] online platform, where an oral bioavailability radar was generated for visual inspection of the physicochemical properties within the spectrum provided by the rules of Lipinski and coauthors [29] and Veber and coauthors [30], in which they include: LIPO ($-0.7 < XlogP3 < 5.0$) [31], SIZE ($150 \text{ g/mol} < MW < 500 \text{ g/mol}$), POLAR ($20 \text{ \AA}^2 < TPSA < 130 \text{ \AA}^2$) [32], INSOLU ($-6 < \log S (\text{ESOL}) < 0$) [33], INSATU ($0.25 < Fsp3 < 1.0$) and FLEX ($0 < nRotb < 9$).

Appropriate physicochemical properties were converted into a quantitative estimate of drug-likeness (QED) [34] as per equation 1, embedded in the ADMETlab 2.0 (<https://admetmesh.scbdd.com/>) [35] online platform, where scores range from 0 (undesirable) to 10 (very desirable).

$$QED = \exp(1/n \sum_{i=1}^n \ln d_i) \quad \text{eq. 1}$$

where n is the number of properties evaluated, which include MW, logP, nHA, nHD, TPSA, nRotb, number of aromatic rings (nAR) and number of undesirable functional groups ($n = 8$), within the desirability parameters (d_i).

The absorption, distribution, metabolism, and excretion (ADME) profile were predicted through the correlation between in silico values and in vitro dataset models, adapted from the methodology by Rocha and coauthors [36]. The molecules were submitted to the predictive test of Brain or Intestinal Estimated Permeation (BOILED-Egg) [37], embedded in the SwissADME (<http://www.swissadme.ch/>) [28] online platform, to predict passive gastrointestinal (GI) and blood-brain barrier (BBB) permeabilities through lipophilicity profiles (WlogP) and polarity (TPSA), as well as substrates and non-substrates of the efflux P-glycoprotein and inhibitors and non-inhibitors of the CYP450 isoenzymes. While in vitro models of permeability in colorectal adenocarcinoma cells (Caco2) and Madin-Darby canine kidney cells (MDCK), as well as the plasma protein binding (PPB), were predicted in the ADMETlab 2.0 platform (<https://admetmesh.scbdd.com/>) [35].

Predictive oral acute toxicity

The possible harm caused by ingestion of the substances was predicted by the quantitative estimate of the lethal dose (LD₅₀) in oral rats, from the self-consistent QSAR regression of the applicability domain of the GUSAR Online platform (<http://www.way2drug.com/gusar/acutopredict.html>) [38].

RESULTS AND DISCUSSION

The *in silico* tests carried out with bixin and six other compounds derived from bixin: annatto, crocetin dimethyl ester, ethyl bixin, mycorradicin, norbixin and transcrocetin (Figure 1), allowed to analyze patterns of binding and coupling between the ligands and the viral proteins NS2B-NS3 and NS5.

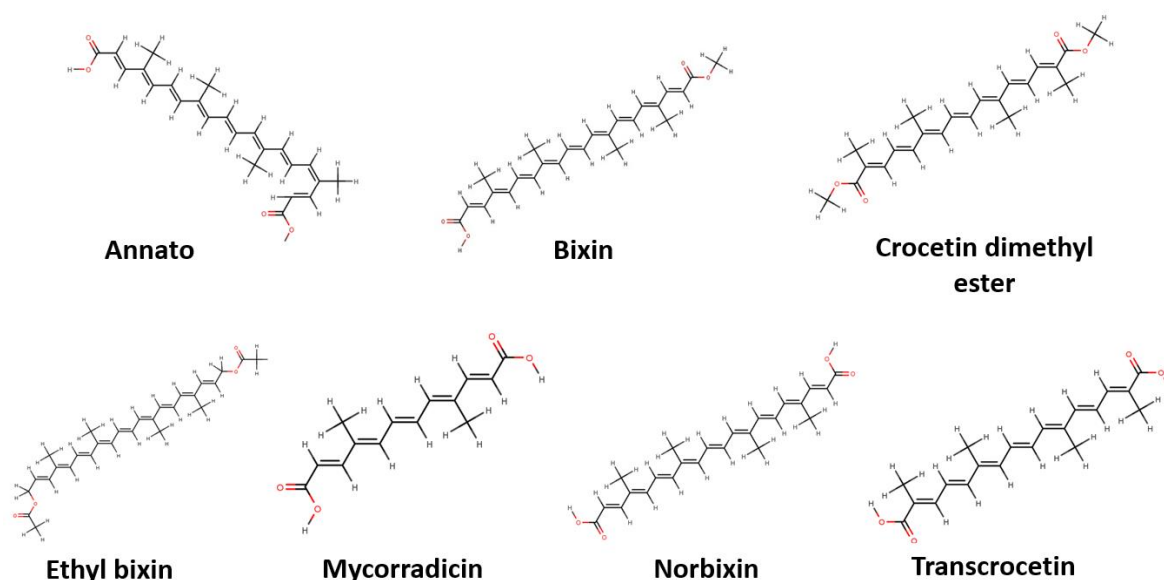


Figure 1. Representation of the chemical structure of bixinoids used in molecular docking assays.

From the analysis of the binding and RMSD energies for the NS2B-NS3 enzyme, it was possible to observe a variation in the affinity energies from -7.1 to -5.5 kcal/mol (Table 1), with values found within the standard of -6.0 kcal/mol or lower ($\Delta G < -6.0$ kcal/mol) [39]. All bixinoid compounds showed interaction with NS2B-NS3 and NS5 S proteases.

Table 1. Molecular fit parameters of bixinoids ligands and NS2B-NS3 protease.

NS2B-NS3	Ligand	RMSD (Å)	Affinity (kcal/mol)
	6T8		
	Annatto	1.237	-5.9
	Bixin	1.880	-6.0
	Crocetin dimethyl ester	1.756	-6.0
	Ethyl Bixin	2.076	-6.0
	Mycorradicin	1.450	-5.5
	Norbixin	2.958	-7.1
	Transcrocetin	1.883	-6.6

When comparing the distances of protein and ligand residues, the best interactions were observed with the NS2B-NS3 protease enzyme. Bixin and ethyl bixin (Figure 2) were the bixinoids that exhibited coupling with the enzyme site in the same region as the 6T8 complexed ligand, although the analysis of the distances with the amino acid residues that constitute the catalytic site of the enzyme showed (Table 2) only some amino acid residues with close distances compared to 6T8.

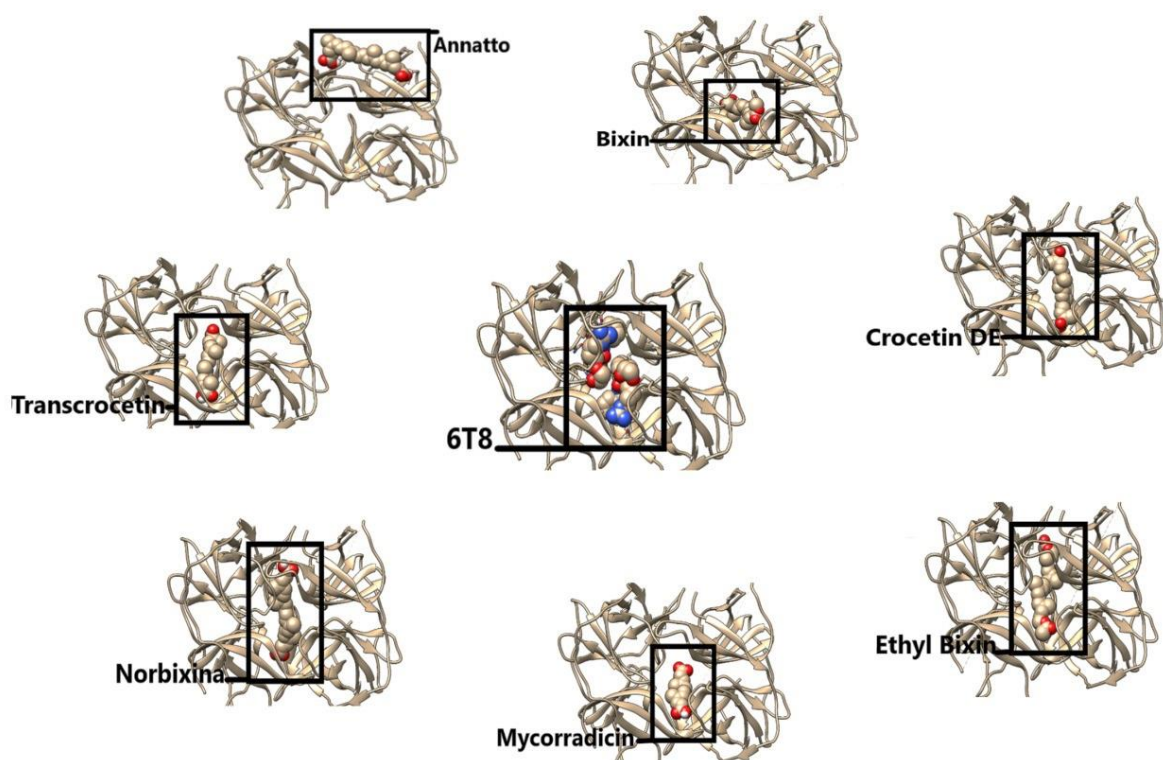


Figure 2. Schematic 2-D representations the docking between NS2B-NS3 protease with 6T8 Inhibitor and bixinoids.

The molecular docking interaction analyzes in the Autodock Vina software for the bixin molecule showed only interactions with three residues: His1051 (4.3 Å) residue belonging to the catalytic triad (His1051, Asp1075 and Ser1135), Asp1075 (3.9 Å) and Ser81 (4.4 Å). Three interactions were observed between the ethyl bixin molecule and the His1051 (4.3 Å) residues belonging to the catalytic triad (His1051, Asp1075 and Ser1135), Asp1075 (3.9 Å) and Asp83 (3.5 Å).

Table 2. Distances of binding residues/NS2B-NS3 protease.

NS2B-NS3	6T8	Annatto	Bixin	Crocetin dimethyl ester	Ethyl Bixin	Mycorradicin	Norbixin	Transcroctin
Ser1135	1,6Å	19.0Å	8.0Å	6.0Å	5.7Å	6.2Å	4.1Å	5.6Å
His1051	3.9 Å	15.1Å	4.3Å	5.3Å	3.5Å	3.0Å	4.4Å	3.3Å
Asp1075	2.9Å	16.4Å	3.9Å	10.5Å	3.0Å	3.4Å	9.0Å	3.8Å
Ser 81	3,0Å	24.0Å	4.4Å	13.4Å	5.9Å	6.5Å	13.3Å	2.8Å
Asp83	2.5Å	25.0Å	10.0Å	8.7 Å	3.5Å	2.9Å	9.4Å	2.7Å

Based on the simulation that showed the shortest distance between the ligand (bixinoid) and the catalytic site of the enzyme, it was possible to identify and evaluate the interactions between bixinoids and NS2B-NS3, being possible to identify two interactions of the *Pi-Alkyl* type with Trp1050 and Tyr1161 and the bixin molecule and an interaction of the *Alkyl* type with Val1072 (Figure 3). The analysis of interactions with the ethyl bixin molecule allowed the identification of two interactions of the *Pi-Alkyl* type with Trp1050 and His1051 and an interaction of the *Alkyl* type with Lys1054, indicating an important route of inhibition (Figure 4).

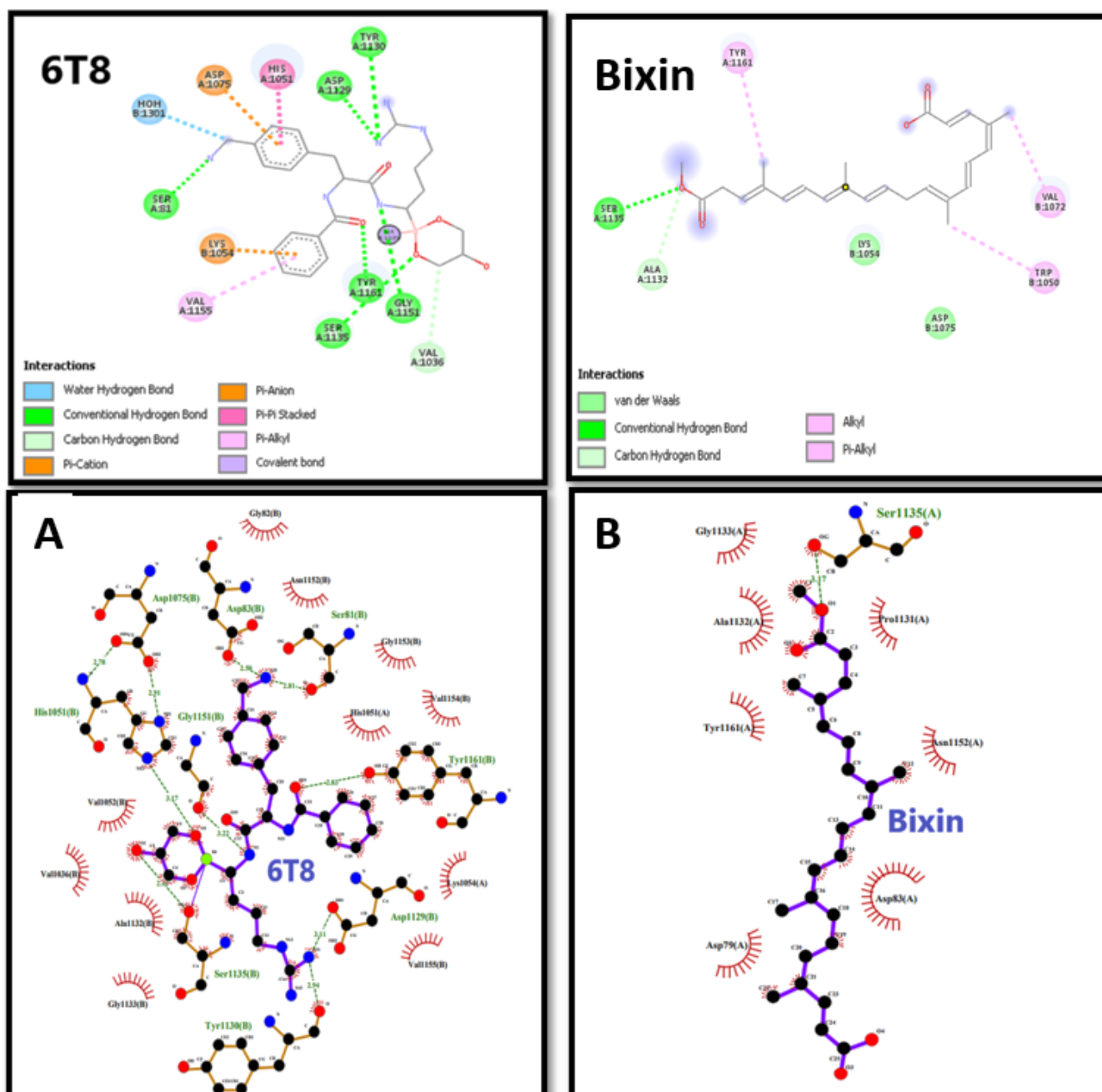


Figure 3. Amino acid interactions between NS2B-NS3 protease and the ligand bixin. Schematic 2-D representations of NS2B-NS3 protease -6T8 complex (A); and NS2B-NS3 protease -bixin complex.

In a previous study that investigated the *in vitro* and *in silico* antiviral activities of the beta-caryophyllene sesquiterpene, present in the essential oil of several aromatic plants, the molecular interaction of sesquiterpene with non-structural ZIKV proteins was observed, whose docking scores were -6.9 kcal/mol and -6.3 kcal/mol, for interactions with binding sites of the NS2B-NS3 and NS5 proteins, respectively [40]. This result obtained by *in silico* assay was confirmed by *in vitro* assays performed with ZIKV in Vero cell culture. Thus, this affinity energy pattern was observed in this study, with better scoring values for bixin and ethyl bixin. A study by Yadav and coauthors [41] demonstrated an interaction between flavonoids and the NS2B-NS5 protease of ZIKV, whose scoring values ranged from -12.13 to 2.13 kcal/mol.

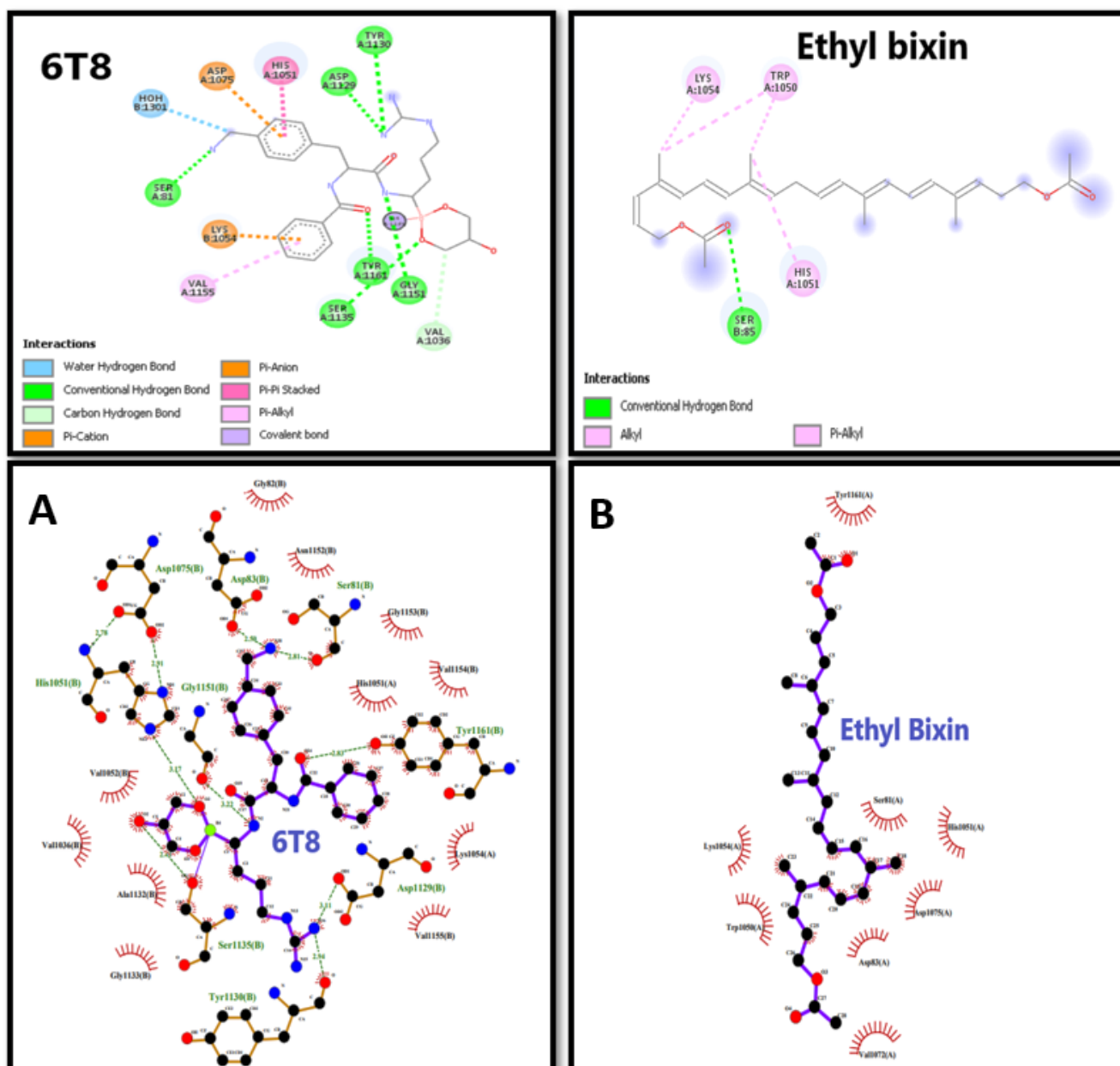


Figure 4. Amino acid interactions between NS2B-NS3 protease and the ligand ethyl bixin. Schematic 2-D representations of NS2B-NS3 protease -6T8 complex (A); and NS2B-NS3 protease -ethyl bixin complex.

The crystalline structure of the NS2B-NS3 enzyme with PDB ID: 5LC0, reveals that NS2B can be found in two conformations; one closed, when attached to a substrate, forming a β -hairpin, close to the binding site of the NS3 protease substrate; one open when it is not interacting with inhibitor or substrate [42]. The NS2B interaction with the NS3 protease facilitates the cleavage of the NS3-mediated viral polyprotein, acting as an important cofactor for the NS3 protease activity [43].

However, the active site of NS2B-NS3 is very well preserved amongst flaviviruses, which points out as a good molecular target in the development of antiviral drugs with a spectrum of action for ZIKV and other viruses from the family Flaviviridae [44, 45], such as the viruses that cause dengue (DENV), West Nile fever (WNV) and yellow fever (YFV).

Molecular screening studies have identified several molecules with antiviral action, targeting the complex NS2B-NS3, such as the study with hydroxychloroquine [46], bromocriptine [47], boronic acid [42] and with several small synthetic molecules [48]. All these studies point to the potential to use NSB-NS3 as an anti-ZIKV molecular target.

In the study for both enzymes, the bixinoid annato was coupled at a site most distant from that used by the respective co-crystallized ligands 6T8 and SAM, from the enzymes NS2B-NS3 protease and NS5 methyltransferase.

For assays with the NS5 enzyme, affinity energies of -6.1 to -4.4 kcal/mol were observed (Table 3). Except for the values found for norbixin and ethyl bixin, all fittings showed values below the standard of up to 2.0 Å for RMSD [25].

Table 3. Molecular fit parameters of bixinoids ligands and NS5 methyltransferase.

NS5	Ligand	RMSD (Å)	Affinity (kcal/mol)
	SAM	0.520	
	Annatto	1.746	-5.0
	Bixin	1.857	-5.7
	Crocetin dimethyl ester	1.761	-4.4
	Ethyl Bixin	2.757	-5.0
	Mycorradicin	1.860	-5.9
	Norbixin	2.152	-6.1
	Transcrocetin	1.745	-6.1

Coupling analysis with the NS5 methyltransferase enzyme, it was observed that the molecules bixin and ethyl bixin (Figure 5) showed the best interactions with the enzyme site in the same region of the complexed ligand S-adenosylmethionine (SAM), suggesting these molecules may represent a potential inhibitor.

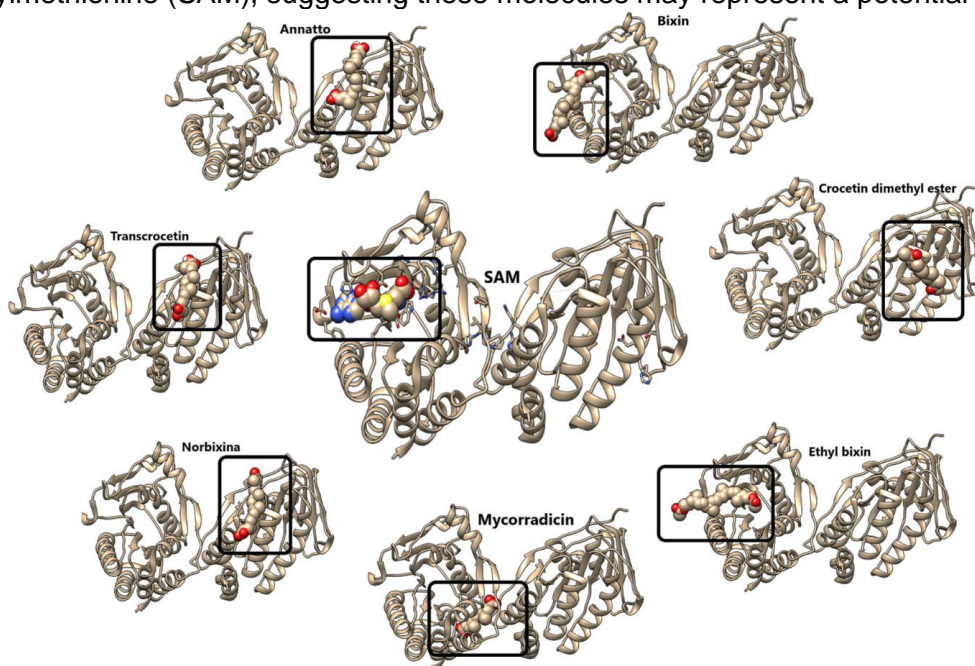


Figure 5. Schematic 2-D representations the docking between NS5 methyltransferase with SAM Inhibitor and bixinoids.

A better interaction was observed for both bixin and ethyl bixin between four amino acid residues (Table 4), Phe 139 (3.6 Å), Ile 153 (4.2 Å), Asp 137 (4.4 Å) and Lys 111 (3.6 Å).

Table 4. Distances of binding residues/NS5 methyltransferase.

NS5	SAM	Annatto	Bixin	Crocetin dimethyl ester	Ethyl Bixin	Mycorradicin	Norbixin	Transcrocetin
Val 138	3.1 Å	47.4 Å	5.5 Å	60.5 Å	5.9 Å	28.3 Å	50.6 Å	52.6 Å
Phe 139	3.2 Å	46.6 Å	3.6 Å	59.7 Å	4 Å	23.1 Å	50 Å	52.1 Å
Ile 153	4.2 Å	40 Å	4.2 Å	57.3 Å	4.6 Å	21.7 Å	47.2 Å	48.2 Å
Asp 137	3.1 Å	49.9 Å	4.4 Å	62.3 Å	4 Å	28.6 Å	53.2 Å	54.2 Å
Lys 111	4.4 Å	45.6 Å	3.6 Å	58.2 Å	5.5 Å	30 Å	51.6 Å	51.1 Å
Ser62	2.7 Å	31.1 Å	9.8 Å	44.5 Å	9.5 Å	22.2 Å	33.2 Å	32.8 Å
Trp93 e	3.2 Å	35.4 Å	10.5 Å	50.2 Å	7.4 Å	15 Å	41.5 Å	40.6 Å
Asp152	2.9 Å	35.9 Å	5.7 Å	49.9 Å	5 Å	15.3 Å	39.4 Å	40.5 Å

Coupling routines with the NS5 methyltransferase generated nine interactions between the NS5 amino acid residues and the bixin molecule (Figure 6), six of which are *Alkyl* type with Val162, Ala165, Arg166, Arg169 and Val170, and two *Pi-Alkyl* interactions with Phe139.

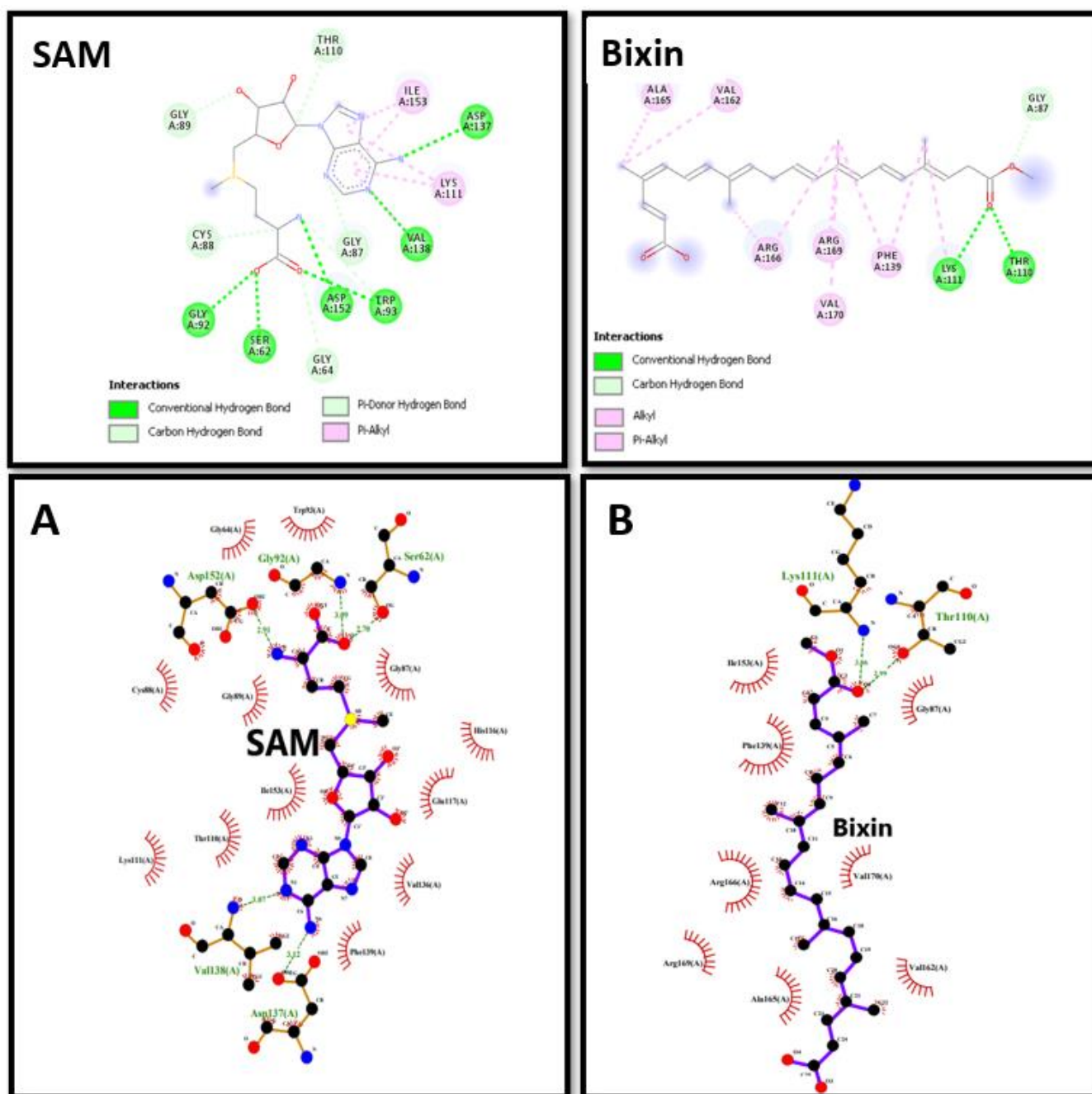


Figure 6. Amino acid interactions between NS5 methyltransferase and the ligand bixin. Schematic 2-D representations of NS5 methyltransferase -SAM complex (A); and NS5 methyltransferase -bixin complex.

Regarding interactions with the ethyl bixin molecule (Figure 7), four interactions were found between NS5 amino acid residues, three of which are *Alkyl* type with Lys111, Ala165, Arg166, Arg169 and Val170, and a *Pi-Alkyl* interaction with Phe139.

After analyzing the results of the interaction between the ligand binding sites, it was possible to observe that bixin and ethyl bixin were coupled to the same chain as the ZIKV NS2B-NS3 and NS5 proteins, when compared to the respective 6T8 and SAM inhibitors. Bixin has low toxicity in animal models [49] and its use has been reported to sensitize cutaneous melanoma tumor cells [50, 51]. Low toxicity is an important point for the development of drugs, in order to avoid possible adverse effects, when clinical administration.

NS5 non-structural protein is the largest product encoded by viral RNA, with about 904 amino acids in the structural composition [52], approximately 100 kDa. NS5 is a bifunctional protein that has two domains:

N terminal domain, which possess methyltransferase (MTase) activity promoting RNA capping, connected via a linker to another C-terminal domain with RNA polymerase (RdRp) activity [53, 54].

ZIKV NS5 methyltransferase is an important target in screening for new molecules that have an inhibitory effect on the action of this enzyme, as reported in previous studies who identified the molecules ZINC1652386 [55], and N, N'-Carbazoyl-aryl-urea [56], both as target molecules for the development of anti-ZIKV drugs.

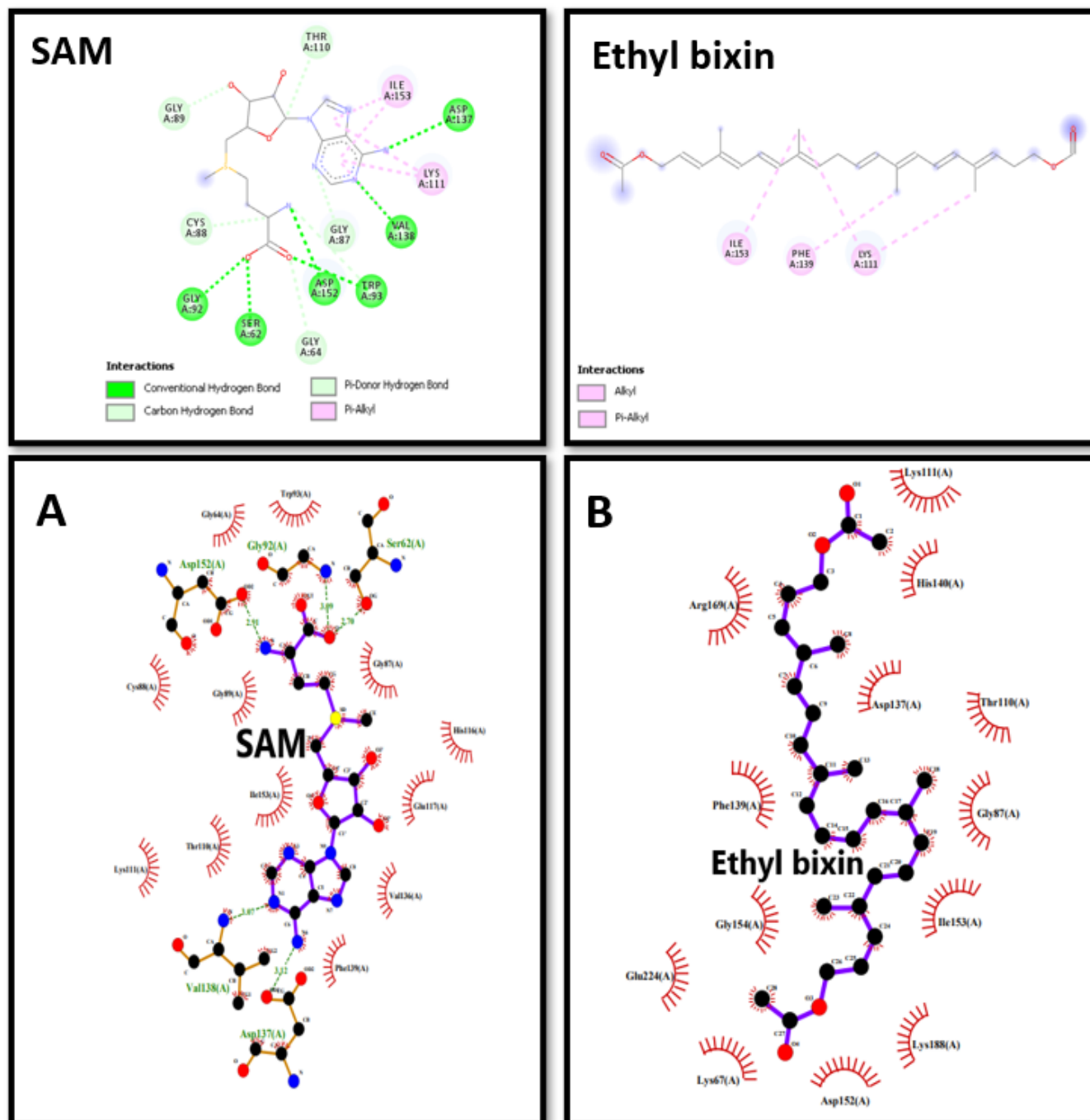


Figure 7. Amino acid interactions between NS5 methyltransferase and the ligand ethyl bixin. Schematic 2-D representations of NS5 methyltransferase -SAM complex (A); and NS5 methyltransferase -ethyl bixin complex.

In rational drug planning, the “rule of five” (ROF) by Lipinski and coauthors [29] is often used to delimit the space of compounds with the greatest number of conditions satisfied to be an oral drug. Parameters include $MW \leq 500$ g/mol, $\log P \leq 5$, number of hydrogen acceptors ($nHA \leq 10$) and hydrogen donors ($nHD \leq 5$) where there is a high probability that a compound is a drug. So, also, with the experimental parameters of the rule of Veber and coauthors [30], which consider the limits between polarity ($TPSA \leq 140 \text{ \AA}^2$) and flexibility ($nRotb \leq 10$) where there is a high probability of good oral bioavailability in rats, as a predictive method of

oral bioavailability in humans. Thus, the measurable drug-likeness properties of a substance can be quantified in terms of its drugability, as shown in equation 1 [34].

According to the bioavailability radar in Figure 8, it is possible to observe that mycorradicin has the lowest lipophilicity evaluated by the XlogP3 method in the order of 3.38 within the predicted drug-likeness spectrum (pink region), due to its small molecular size (MW = 248.27 g/mol) and the polarity of 74.60 Å² associated with its two carboxyl groups. It is noteworthy that the substances bixin and ethyl bixin do not meet the ideal characteristics for good oral bioavailability, since they are very lipophilic and flexible, at the same time as having the best drugability scores associated with the substances mycorradicin and transcrocetin, in the order of 0.560 and 0.504, respectively, suggest a good bioavailability for interaction with NS2B-NS3 and NS5 proteins, as they better meet the conditions established by ROF [57] (Table 5).

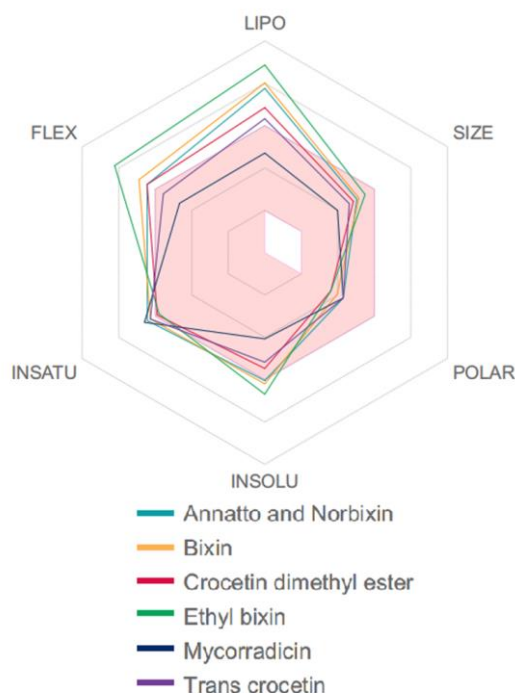


Figure 8. Bioavailability radar plotted by the drug-likeness parameters of these bixinoids.

The *in silico* predictive method of Brain or Intestinal Estimated permeation (BOILED-Egg), built into the SwissADME platform, has assisted pharmaceutical chemists in the instant screening of new drug candidates. Based on the physicochemical descriptors of lipophilicity (WlogP) and polarity (TPSA), the tool can show possible drugs well absorbed in the human intestine and with activity in the central nervous system (CNS) due to permeability in the blood-brain barrier (BBB) [37]. Together with the dataset of *in vitro* parameters of permeability in colorectal adenocarcinoma cells (Caco2) and Madin-Darby canine kidney cells (MDCK), as well as the degrees of affinity with plasma proteins, built into the ADMETlab 2.0 [35] platform, it was possible to establish a consensual correlation on the absorption and systemic distribution of bixin analogues.

Table 5. Physical-chemical and medicinal properties of these bixinoids.

	Annato	Bixin	Crocetin dimethyl ester	Ethyl bixin	Mycorradicin	Norbixin	Transcrocetin
MW	380.48	394.50	356.46	436.58	248.27	380.48	328.40
XlogP3	7.20	7.52	6.06	8.58	3.38	7.20	5.41
WlogP	5.72	5.81	4.79	6.68	2.72	5.72	4.61
nHA	4	4	4	4	4	4	4
nHD	2	1	0	0	2	2	2
TPSA	74.60	63.60	52.60	52.60	74.60	74.60	74.60
nRotb	10	11	10	14	6	10	8
Fsp3	0.17	0.20	0.27	0.29	0.14	0.17	0.20
RO5	Yes	Yes	Yes	Yes	Yes	Yes	Yes
Veber	Yes	No	Yes	No	Yes	Yes	Yes
QED	0.375	0.288	0.357	0.194	0.560	0.375	0.504

The BOILED-Egg (Figure 9) shows that the substances mycorradicin and trans crocetin are within the predicted spectrum for a predicted high gastrointestinal (GI) permeability ($TPSA < 142 \text{ \AA}^2$ and $-2.3 < WlogP < 6.8$), with logarithmic coefficients of permeability in Caco2 cells in the order of -5.5 cm/s and close to ideal for high intestinal permeability ($\log PCaco2 > 5.15 \text{ cm/s}$) [58].

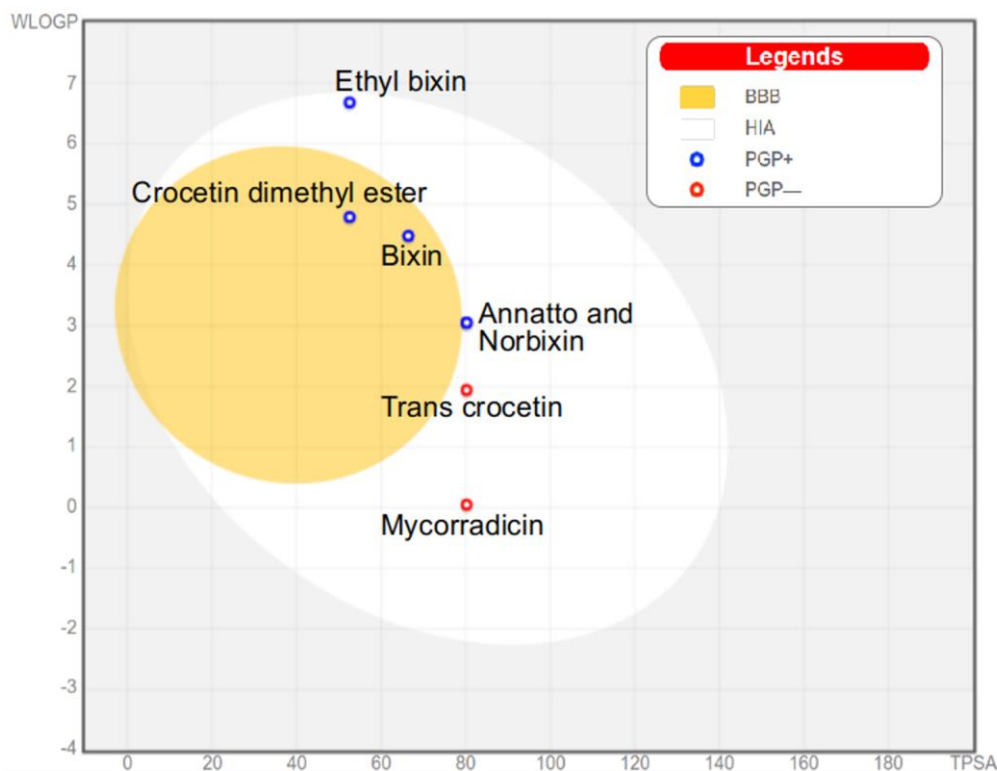


Figure 9. Passive permeation in the human intestine and blood-brain barrier of these ligands.

However, they ensure greater bioavailability as they are not P-glycoprotein (P-gp) substrates, contrary to what happens with annatto and norbixin, which are loaded at physiological pH and undergo efflux back to the GI tract because they are substrates of P-gp, in addition to having a high degree of affinity with plasma proteins ($> 96\%$), which reduces their free volumes for distribution in the systemic circulation (Table 6).

Table 6. Predicted ADME properties by the in silico and in vitro models of SwissADME e ADMETlab 2.0.

	Annatto	Bixin	Crocetin dimethyl ester	Ethyl bixin	Mycorradicin	Norbixin	Transcrocetin
GI permeation	High	High	High	High	High	High	High
$\log P_{Caco2}$	-5.43	-5.12	-4.94	-5.13	-5.51	-5.55	-5.51
P-gp substrate	Yes	Yes	Yes	Yes	No	Yes	No
$Papp$ (MDCK)	8.1×10^{-6}	1.3×10^{-5}	1.7×10^{-5}	1.6×10^{-5}	5.0×10^{-6}	8.9×10^{-6}	1.1×10^{-5}
BBB permeation	No	Yes	Yes	No	No	No	No
%PPB	96.82	97.22	90.61	99.33	83.18	96.56	92.92
CYP1A2 inhibitor	No	No	No	No	No	No	No
CYP2C19 inhibitor	No	No	Yes	No	Yes	No	Yes
CYP2C9 inhibitor	No	Yes	Yes	Yes	No	No	No
CYP2D6 inhibitor	No	No	No	No	No	No	No
CYP3A4 inhibitor	No	No	No	No	No	No	No

The activity in the CNS was evaluated in a systematic analysis of the graph in Figure 9 and Table 6, where it is possible to observe that the apparent permeability coefficients (P_{app}) of the MDCK model $> 1.0 \times 10^{-5}$ cm/s, associated with the substances bixin, crocetin dimethyl ester, ethyl bixin and transcrocetin reflect the high permeability in the BBB [59], with the substances bixin and crocetin dimethyl ester within the ideal spectrum predicted for a passive cerebral permeability through the BBB ($TPSA < 79 \text{ \AA}^2$ and $0.4 < WlogP < 6.0$). However, it is worth noting that bixin and ethyl bixin are substrates of P-gp, which limits their access to the CNS as they undergo efflux to the external environment of the BBB, increasing their concentrations in the adjacent blood, where their affinities with plasma proteins are greater than 97%. It is also worth noting that transcrocetin is a charged compound and has about 92% of its molar volume bound to plasma proteins, which tends to decrease its free molecular fraction to penetrate the BBB but tends to be active in the CNS due to low passive efflux across biological membranes.

Through the fragmenting method of Veith and coauthors [60] it was possible to relate the molecular fragments of substances with the inhibitions and non-inhibitions of the cytochrome P450 (CYP450) isoenzymes predicted by the datasets of the SwissADME platform, since this class of enzymes is responsible for the oxidation-reduction reactions of xenobiotics in phase I metabolism.

The substances have a high susceptibility to be substrate of most CYP450 isoenzymes with a strong contribution from their carboxylate groups and derivatives, where it is possible to highlight the substances annatto and norbixin as non-inhibitors of the evaluated enzyme families (1A2, 2C19, 2C9, 2D6 and 3A4), while the substances bixin, crocetin dimethyl ester, ethyl bixin, mycorradicin and transcrocetin have a tendency to inhibit the CYP2C isoenzyme family, which may result in a higher plasma concentration of these substances after first-pass metabolism [61] (Table 6).

Acute toxicity in rodents constitutes a predictive method frequently used in the discovery of new drugs with low toxicological risk. In this study, lethal dose values (LD_{50}) were predicted for toxic effects by oral administration in rats, as a predictive method of acute oral toxicity in humans. For this, the GUSAR Online server has its applicability domain that uses a self-consistent QSAR regression based on the electrotopological neighborhoods of atoms (QNA) to relate the molecular structure with possible toxic risks by ingestion [38].

Thus, it is possible to observe that the substances crocetin dimethyl ester and ethyl bixin obtained the best results for acute toxicity. Substances are non-charged at physiological pH and LD_{50} values in the order of 8218 and 9450 mg/kg, crocetin dimethyl ester and ethyl bixin respectively, are considerably high and do not present a toxic risk by ingestion. Despite the excellent results of these two substances, the other molecules, including those with better oral bioavailability: mycorradicin and trans crocetin, have their predicted values of $LD_{50} > 2000$ mg/kg, which means that the structural contributions of these substances suggest that they do not tend to be toxic by oral administration (Figure 10) [62], constituting promising therapeutic strategies in the treatment of Zika Virus.

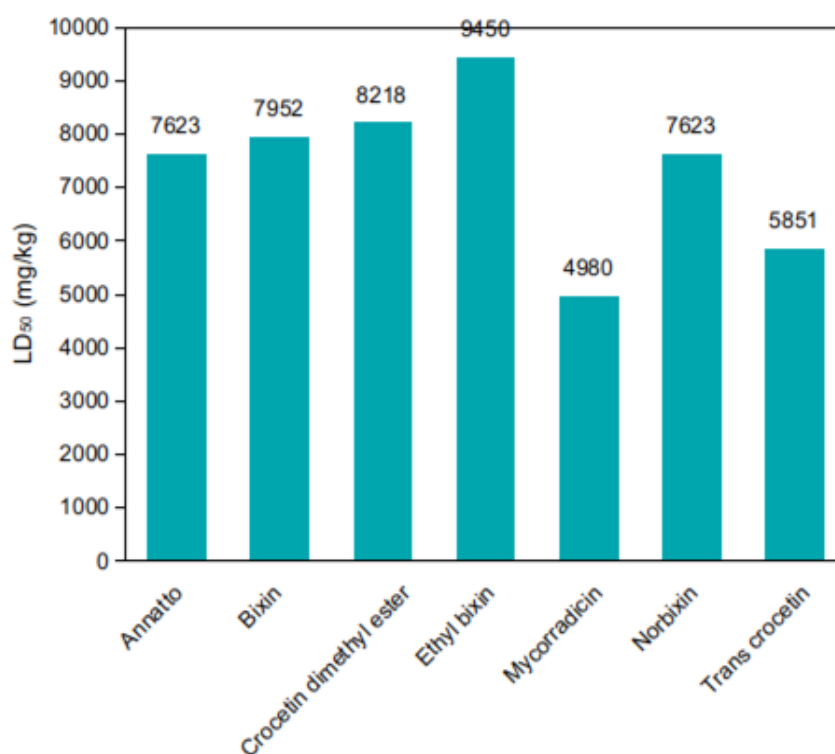


Figure 10. Predicted LD₅₀ of these bixinoids by the QSAR models of GUSAR Online tool.

Recent studies point to the importance of viral RNA methylation in the process of multiplication and infectivity of ZIKV and other flaviviruses, such as DENV, YFV, and JEV [52, 63, 64]. The results obtained by molecular docking assay, point to affinity between the bixinoid binding sites with NS5 methyltransferase, which suggests a possible inhibitory effect on the viral replication process, as NS5 influences the virus life cycle on genome replication, interferon capping and suppression, through immune system evasion mechanisms [65].

CONCLUSION

In silico molecular docking assays are promising in elucidating possible mechanisms of molecular interaction between pharmacologically active substances and binding sites for pharmacological targets, such as non-structural virus proteins. Since the only epidemiological control measures for Zika fever are vector control and health education, the development of antiviral drugs is a necessity, especially for the treatment of arboviruses. Among the seven bixinoid compounds, bixin and ethyl bixin exhibited better patterns of interaction with amino acid residues present in the catalytic site of both NS2B-NS3 protease and NS5 methyltransferase enzymes, that is, they interacted in the region close to the site occupied by the 6T8 and SAM inhibitors, already complexed with the enzymes NS2B-NS3 protease and NS5 methyltransferase, respectively. Physicochemical properties of bixinoids suggest a good oral bioavailability of the substances mycorradicin and transcrocetin, since they have high passive gastrointestinal permeability and the lowest binding to plasma proteins in this study, which ensure a good molecular volume available for interaction with ZKV targets without toxic risk by ingestion. These molecules are promising as antiviral agents, inhibitors of key enzymes in the ZIKV replication cycle. on viral growth. However, *in vitro* biological studies are necessary to investigate biochemical and pharmacological parameters of these molecules.

Acknowledgments: The authors thanks Coordenação de Aperfeiçoamento de Pessoal de Nível Superior (CAPES) and Conselho Nacional de Desenvolvimento Científico e Tecnológico (CNPq) for the financial support.

Conflict of interest: The authors declare no conflict of interest.

REFERENCES

1. Weaver SC, Costa F, Garcia-Blanco MA, Ko AI, Ribeiro GS, Saade G, et al. Zika virus: history, emergence, biology, and prospects for control. *Antiviral Res.* 2016;130:69–80.
2. Cao-Lormeau VM, Blake A, Mons S, Lastère S, Roche C, Vanhomwegen J, et al. Guillain-Barré Syndrome outbreak associated with Zika virus infection in French Polynesia: a case-control study. *The Lancet.* 2016;387:1531-9.
3. Rasmussen SA, Jamieson DJ, Honein MA, Petersen LR. Zika virus and birth defects—reviewing the evidence for causality. *N Engl J Med.* 2016;374(20):1981-7.
4. Duffy MR, Chen TH, Hancock WT, Powers AM, Kool JL, Lanciotti RS, et al. Zika virus outbreak on Yap Island, federated states of Micronesia. *N Engl J Med.* 2009;360(24):2536-43.
5. Cao-Lormeau VM, Roche C, Teissier A, Robin E, Berry AL, Mallet HP, et al. Zika virus, French Polynesia, South Pacific, 2013. *Emerg Infect Dis.* 2014;20(6):1085-86.
6. Paixão ES, Barreto F, Teixeira MG, Costa MCN, Rodrigues LC. History, epidemiology, and clinical manifestations of Zika: a systematic review. *Am J Public Health.* 2016;106(4):606-12.
7. Cardoso CW, Paploski IA, Kikuti M, Rodrigues MS, Silva MM, Campos GS, et al. Outbreak of exanthematous illness associated with Zika, chikungunya, and dengue viruses, Salvador, Brazil. *Emerg Infect Dis.* 2015;21(12):2274-6.
8. Zanluca C, Melo VCA, Mosimann ALP, Santos GIV, Santos CND, Luz K. First report of autochthonous transmission of Zika virus in Brazil. *Mem Inst Oswaldo Cruz.* 2015;110(4):569-72.
9. Shiryayev SA, Strongin AY. Structural and Functional Parameters of the Flaviviral Protease: A Promising Antiviral Drug Target. *Future Virol.* 2010;5:593–606.
10. Bollati M, Alvarez K, Assenberg R, Baronti C, Canard B, Cook S, et al. Structure and Functionality in Flavivirus NS-Proteins: Perspectives for Drug Design. *Antiviral Res.* 2010;87:125–48.
11. Vilar DA, Vilar MSA, Raffin FN, Oliveira MR, Franco CFO, Athayde-Filho PF, et al. Traditional uses, chemical constituents, and biological activities of *Bixa orellana* L.: a review. *Sci World J.* 2014;1-11.
12. Tay-Agbozo S, Street S, Kispert L. The carotenoid Bixin found to exhibit the highest measured carotenoid oxidation potential to date consistent with its practical protective use in cosmetics, drugs and food. *J Photochem Photobiol B Biol.* 2018;186:1-8.
13. Husa NN, Hamzah F, Said HM. Characterization and Storage Stability Study of Bixin Extracted from *Bixa orellana* Using Organic Solvent. In *IOP. Conf Series: Mater Sci Eng.* 2018;358):1-7.
14. Rincón CTS, Gómez GLC, Montoya JEZ. Extracción de compuestos fenólicos y actividad antioxidante de hojas de *Bixa orellana* L.(achiote). *Rev Cuba Plantas Med.* 2016;21(2):133-44.
15. Khan MA, Jain DC, Bhakuni RS, Zaim M, Thakur RS. Occurrence of some antiviral sterols in *Artemisia annua*. *Plant Sci.* 1991;75(2):161-5.
16. Bernatchez JA, Tran LT, Li J, Luan Y, Siqueira-Neto JL, Li R. Drugs for the treatment of Zika virus infection. *J Med Chem.* 2019;63(2):470-89.
17. Pettersen EF, Goddard TD, Huang CC, Couch GS, Greenblatt DM, Meng EC, et al. UCSF Chimera—a visualization system for exploratory research and analysis. *J. Comput. Chem.* 2004;25(13):1605-12.
18. Sanner MF, Huey R, Dallakyan S, Karnati S, Lindstrom W, Morris GM, et al. AutoDockTools, version 1.4. 5. The Scripps Research Institute, La Jolla. 2007.
19. Trott O, Olson AJ. AutoDock Vina: improving the speed and accuracy of docking with a new scoring function, efficient optimization, and multithreading. *J Comput Chem.* 2010;31(2):455-61.
20. Biovia DS, Berman HM, Westbrook J, Feng Z, Gilliland G, Bhat TN, Richmond TJ. Dassault Systèmes BIOVIA, Discovery Studio Visualizer, v.17.2, San Diego: Dassault Systèmes, 2016. *J Chem Phys.* 2000; 10:0021-9991.
21. Laskowski RA, Swindells MB. LigPlot+: multiple ligand-protein interaction diagrams for drug discovery. *J Chem Inf Model.* 2011;51:2778-86.
22. Halgren TA. Merck molecular force field. I. Basis, form, scope, parameterization, and performance of MMFF94. *J Comput Chem.* 1996;17(5-6):490-519.
23. Meza JC. Steepest descent. *WIRES Comp Stats.* 2010;2(6):719-22.
24. Hanwell MD, Curtis DE, Lonie DC, Vandermeersch T, Zurek E, Hutchison GR. Avogadro: an advanced semantic chemical editor, visualization, and analysis platform. *J cheminformatics.* 2012;4(1):17.
25. Yusuf D, Davis AM, Kleywegt GJ, Schmitt S. An alternative method for the evaluation of docking performance: RSR vs RMSD. *J. Chem. Inf. Model.* 2008;48(7):1411-22.
26. Gaillard T. Evaluation of AutoDock and AutoDock Vina on the CASF-2013 benchmark. *J Chem Inf Model.* 2018;58(8):1697-706.

27. Borowiecki P, Wawro AM, Wińska P, Wielechowska M, Bretner M. Synthesis of novel chiral TBBt derivatives with hydroxyl moiety. Studies on inhibition of human protein kinase CK2 α and cytotoxicity properties. *Eur J Med Chem.* 2014;84:364-74.
28. Daina A, Michielin O, Zoete V, Swiss ADME. A Free Web Tool to Evaluate Pharmacokinetics, Drug- Likeness and Medicinal Chemistry Friendliness of Small Molecules. *Nat Publ Gr.* 2017;7(1):1-13.
29. Lipinski CA, Lombardo F, Dominy BW, Feeney PJ. Experimental and Computational Approaches to Estimate Solubility and Permeability in Drug Discovery and Development Settings. *Adv Drug Deliv Rev.* 1997;23(1-3):3-25.
30. Veber DF, Johnson SR, Cheng HY, Smith BR, Ward KW, Kopple KD. Molecular Properties That Influence the Oral Bioavailability of Drug Candidates. *J Med Chem.* 2002;45(12):2615-23.
31. XLOGP3. Log Po/w: Atomistic and Knowledge-Based Method, XLOGP3 Program Version 3.2.2.
32. Ertl P, Rohde B, Selzer P. Fast Calculation of Molecular Polar Surface Area as a Sum of Fragment-Based Contributions and Its Application to the Prediction of Drug Transport Properties. *J. Med. Chem.,* 2000;43(20):3714-17.
33. Delaney JS. ESOL: estimating Aqueous Solubility Directly from Molecular Structure. *J Chem Inf Comput Sci.* 2004;44(3):1000-5.
34. Bickerton GR, Paolini GV, Besnard J, Muresan S, Hopkins AL. Quantifying the Chemical Beauty of Drugs. *Nat Chem.* 2012;4(2):90-8.
35. Xiong G, Wu Z, Yi J, Fu L, Yang Z, Hsieh C, et al. ADMETlab 2.0: An Integrated Online Platform For accurate and Comprehensive Predictions of ADMET properties. *Nucleic Acids Res.* 2021;1-10.
36. Rocha MN, Alves DR, Marinho MM, Morais SM, Marinho ES. Virtual Screening of Citrus Flavonoid Tangeretin: A Promising Pharmacological Tool for the Treatment and Prevention of Zika Fever and COVID-19. *J Comput Biophys Chem.* 2021;20(03):283-304.
37. Daina A, Zoete V. A BOILED-Egg to Predict Gastrointestinal Absorption and Brain Penetration of Small Molecules. *Chem Med Chem.* 2016;11(11):1117-21.
38. Lagunin A, Zakharov A, Filimonov D, Poroikov V. QSAR Modelling of Rat Acute Toxicity on the Basis of PASS Prediction. *Mol Inform.* 2011;30(2-3):241-50.
39. Shityakov S, Förster C. In silico predictive model to determine vector-mediated transport properties for the blood-brain barrier choline transporter. *Adv Appl Bioinforma. Chem.* 2014;7:23.
40. Sobrinho AC, Morais SM, Marinho MM, Souza NV, Lima DM. Antiviral activity on the Zika virus and larvicidal activity on the *Aedes* spp. of *Lippia alba* essential oil and β -caryophyllene. *Ind Crops Prod.* 2021;162:113281.
41. Yadav R, Selvaraj C, Aarthy M, Kumar P, Kumar A, Singh SK, et al. Investigating into the molecular interactions of flavonoids targeting NS2B-NS3 protease from ZIKA virus through in-silico approaches. *J Biomol Struct.* 2021;39(1):272-84.
42. Lei J, Hansen G, Nitsche C, Klein CD, Zhang L, Hilgenfeld R. Crystal Structure of Zika Virus NS2B-NS3 Protease in Complex with a Boronate Inhibitor. *Science.* 2016;353:503-5.
43. Chen X, Yang K, Wu C, Chen C, Hu C, Buzovetsky O, et al. Mechanisms of Activation and Inhibition of Zika Virus NS2B-NS3 Protease. *Cell Res.* 2016;26:1260-3.
44. Voss S, Nitsche C. Inhibitors of the Zika virus protease NS2B-NS3. *Bioorg Med Chem Lett.* 2020;30(5):126965.
45. Nitsche C. Proteases from dengue, West Nile and Zika viruses as drug targets. *Biophys Rev.* 2019;11(2):157-65.
46. Kumar A, Liang B, Aarthy M, Singh SK, Garg N, Mysorekar IU, et al. Hydroxychloroquine inhibits Zika virus NS2B-NS3 protease. *ACS Omega.* 2018;3(12):18132-41.
47. Chan JF, Chik KK, Yuan S, Yip CC, Zhu Z, Tee KM, et al. Novel antiviral activity and mechanism of bromocriptine as a Zika virus NS2B-NS3 protease inhibitor. *Antivir Res.* 2017;141:29-37.
48. Lee H, Ren J, Nacadello S, Rice AJ, Ojeda I, Light S, et al. Identification of novel small molecule inhibitors against NS2B/NS3 serine protease from Zika virus. *Antivir Res.* 2017;139:49-58.
49. Stohs SJ. Safety and efficacy of *Bixa orellana* (achiote, annatto) leaf extracts. *Phytother Res.* 2014;28(7):956-60.
50. Júnior RGO, Bonnet A, Braconnier E, Groult H, Prunier G, Beaugeard L, et al. Bixin, an apocarotenoid isolated from *Bixa orellana* L., sensitizes human melanoma cells to dacarbazine-induced apoptosis through ROS-mediated cytotoxicity. *Food Chem Toxicol.* 2019;125:549-61.
51. Bautista AR, Moreira EL, Batista MS, Miranda MS, Gomes IC. Subacute toxicity assessment of annatto in rat. *Food Chem Toxicol.* 2004;42(4):625-9.
52. Elishahawi H, Syed Hassan S, Balasubramaniam V. Importance of Zika virus NS5 protein for viral replication. *Pathogens.* 2019;8(4):169-81.
53. Piorkowski G, Richard P, Baronti C, Gallian P, Charrel R, Leparç-Goffart I, et al. Complete coding sequence of Zika virus from Martinique outbreak in 2015. *New Microbes New Infect.* 2016;11:52–3.

54. Zhao B, Yi G, Du F, Chuang YC, Vaughan RC, Sankaran B, et al. Structure and function of the Zika virus fulllength NS5 protein. *Nat Commun.* 2017;8:1-9.
55. Santos FR, Lima WG, Maia EH, Assis LC, Davyt D, Taranto AG, et al. Identification of a potential Zika Virus inhibitor targeting NS5 methyltransferase using virtual Screening and molecular dynamics simulations. *J Chem Inf Model.* 2020;60(2):562-8.
56. Spizzichino S, Mattedi G, Lauder K, Valle C, Aouadi W, Canard B, et al. Design, Synthesis and Discovery of N, N'-Carbazoyl-aryl-urea Inhibitors of Zika NS5 Methyltransferase and Virus Replication. *ChemMedChem.* 2020;15(4):385.
57. Lipinski CA. Rule of Five in 2015 and beyond: Target and Ligand Structural Limitations, Ligand Chemistry Structure and Drug Discovery Project Decisions. *Adv Drug Deliv Rev.* 2016;101:34-41.
58. Wang NN, Dong J, Deng YH, Zhu MF, Wen M, Yao ZJ, et al. ADME Properties Evaluation in Drug Discovery: Prediction of Caco-2 Cell Permeability Using a Combination of NSGA-II and Boosting. *J Chem Inf. Model.* 2016 56(4):763-73.
59. Silverman RB, Holladay MW. Lead Discovery and Lead Modification. In *The organic chemistry of drug design and drug action*; Academic Press Inc. 2014;81-2.
60. Veith H, Southall N, Huang R, James T, Fayne D, Artemenko N, et al. Comprehensive Characterization of Cytochrome P450 Isozyme Selectivity across Chemical Libraries. *Nat Biotechnol.* 2009;27(11):1050-5.
61. Eitrich T, Kless A, Druska C, Meyer W, Grotendorst J. Classification of Highly Unbalanced CYP450 Data of Drugs Using Cost Sensitive Machine Learning Techniques. *J Chem Inf Model.* 2007;47(1):92-103.
62. Diaza RG, Manganelli S, Esposito A, Roncaglioni A, Manganaro A, Benfenati E. Comparison of in Silico Tools for Evaluating Rat Oral Acute Toxicity. *SAR QSAR Environ. Res.* 2015;26(1):1-27.
63. Rusanov T, Kent T, Saeed M, Hoang TM, Thomas C, Rice CM, et al. Identification of a Small Interface between the Methyltransferase and RNA Polymerase of NS5 that is Essential for Zika Virus Replication. *Sci Rep.* 2018;8(1):1-1.
64. Dubankova A, Boura E. Structure of the yellow fever NS5 protein reveals conserved drug targets shared among flaviviruses. *Antivir Res.* 2019;169:104536.
65. Wang B, Thurmond S, Hai R, Song J. Structure and function of Zika virus NS5 protein: perspectives for drug design. *Cell Mol Life Sci.* 2018; 75(10):1723-36.



© 2022 by the authors. Submitted for possible open access publication under the terms and conditions of the Creative Commons Attribution (CC BY NC) license (<https://creativecommons.org/licenses/by-nc/4.0/>).